Front. Mech. Eng. 2012, 7(1): 81–92
DOI 10.1007/s11465-012-0309-4

RESEARCH ARTICLE

Tie ZHANG, Fan OUYANG

Offline motion planning and simulation of two-robot welding coordination

Abstract This paper focuses on the two-robot welding coordination of complex curve seam which means one robot grasp the workpiece, the other hold the torch, the two robots work on the same workpiece simultaneously. This paper builds the dual-robot coordinate system at the beginning, and three point calibration method of two robots' relative base coordinate system is presented. After that, the non master/slave scheme is chosen for the motion planning, the non master/slave scheme sets the poses versus time function of the point u on the workpiece, and calculates the two robot end effecter trajectories through the constrained relationship matrix automatically. Moreover, downhand welding is employed which can guarantee the torch and the seam keep in good contact condition all the time during the welding. Finally, a Solidworks-SimMechanics simulation platform is established, and a simulation of curved steel pipe welding is conducted. The results of the simulation illustrate the welding process can meet the requirements of downhand welding, the joint displacement curves are smooth and continuous and no joint velocities are out of working scope.

Keywords complex curve seam, two robots, coordinated welding, motion planning

1 Introduction

The research of multi-robot coordination started from early 1980s, represented by two-robot coordination system. The advantages of two-robot system compared with single robot include, at first, it reduces execution time, the second, it adds flexibility in motion optimization, for the third, it maximizes the use of manipulator workspace, finally, it allows tracking of sharp corners using smooth paths [1]. It is a complicated system due to nonlinear characteristics, motion constrains and kinematics redundancy. There are two types of two-robot coordinating operations: tight coordination and loose coordination: Loose coordination and tight coordination. In loose coordination, robots are working in a common workspace and each robot independently executes a task which is unrelated to the tasks of other robots. In tight coordination, robot manipulators coordinately handle a common object in a common workspace [2]. Only kinematics coordination is needed for the loose coordination while tight coordination need to consider both kinematics and dynamics coordination at most of time.

For the two-robot loose coordination. Most of the research is focused on the two-robot collision avoidance and time-optimal motion planning that one robot execute the task independently while the second robot delay the starting time [3–5], reduce speed [3,6] or change the Cartesian path [7,8] to avoid colliding with the former one.

For the tight coordination with contact force, which need to consider both kinematics and dynamics coordination that include compliant coordination [9,10] and hybrid position/force coordination [11,12].

For the tight coordination without contact force, the coordination of arc-welding robot and positioner system is one of the research hotspot [1,13]. However, for two 6-degree-of-freedom (DOF) industrial robot welding coordination that one robot gripping the workpiece to be welded, the other robot holds the torch and implements the welding task, few research can be found. In Ref. [14], the author introduces the coordinated motion constraints in the dual-robot welding teaching process, which only need to teach the master robot, the slave robot can automatically follow the master robot under the motion coordination; this can reduce a large number of teaching operations. The positioner at most has three DOF, while the DOF of two-robot coordinated welding system is increased up to 12 comparatively. Two 6-DOF robot systems can meet the demand of advanced and more complex welding tasks.

Received November 16, 2011; accepted December 14, 2011

Tie ZHANG, Fan OUYANG (✉)
School of Mechanical & Automotive Engineering, South China University of Technology, Guangzhou 510640, China
E-mail: oooyyyffff@hotmail.com

This paper studies two 6-DOF robots coordination, the three-point calibration method is first given to obtain the base coordinate system transformation matrix between two robots. After that, the non-mater/slave approach is employed which specifies the time versus pose function of a point u on a given workpiece, the end effecter paths of both robots can be obtained by the motion constrains respectively. Finally a two-robot coordinated welding Solidworks-SimMechanics simulation platform is established, and a coordinated welding simulation of a steel curved pipe used in petrochemical and coal industry is given.

2 Dual-robot coordinate system and calibration

2.1 Establishment of dual-robot coordinate system

$i = 1$ indicates the welding robot, $i = 2$ indicates the clamping robot. $[R_i]$ represent the robot base coordinate system, $[E_i]$ represents the robot end-effecter coordinate system, $[u]$ represents the workpiece coordinate system, $[T_i]$ represents the tool end coordinate system.

${}^{R_i}\boldsymbol{T}_{E_i}$ indicates the transformation matrix from $[E_i]$ to $[R_i]$.

${}^{E_i}\boldsymbol{T}_{T_i}$ indicates the transformation matrix from $[T_i]$ to $[R_i]$.

${}^{R_1}\boldsymbol{T}_{R_2}$ indicates the transformation matrix from $[R_2]$ to $[R_1]$.

${}^{T_i}\boldsymbol{T}_u$ indicates the transformation matrix from $[u]$ (point u on the workpiece) to $[T_i]$.

$\boldsymbol{T}_u$ indicates the pose versus time function matrix of $[u]$ in the R_1 coordinate system.

According to the kinematics transformation relationship, as indicated in Fig. 1, the coordinate constraint relationship between Robot1 and Robot2 can be expressed as follow:

$$
\begin{aligned}
&{}^{R_1}\boldsymbol{T}_{E_1} \times {}^{E_1}\boldsymbol{T}_{T_1} \times {}^{T_1}\boldsymbol{T}_u \\
&= {}^{R_1}\boldsymbol{T}_{R_2} \times {}^{R_2}\boldsymbol{T}_{E_2} \times {}^{E_2}\boldsymbol{T}_{T_2} \times {}^{T_2}\boldsymbol{T}_u = \boldsymbol{T}_u. \qquad (1)
\end{aligned}
$$

${}^{R_i}\boldsymbol{T}_{E_i}$ is unknown that can be calculated by the 6 joint angular displacements. ${}^{E_i}\boldsymbol{T}_{T_i}$ is decided by the assembly of the robot end-effecter and the tool; $\boldsymbol{T}_u$ is specified by the robot operator; ${}^{U}\boldsymbol{T}_{T_i}$ is obtained by the motion constraint relationship. These three transformation matrixes are already known. The unknown matrix ${}^{R_1}\boldsymbol{T}_{E_2}$ can be obtained through calibration, which is decided by the relative positioning between the two robots.

2.2 Three-point calibration method of two robots' relative base coordinate system

The relative pose calibration method between two robot's base coordinate system is modified based on the calibration method used between welding robot and positioner [15].

Before the calibration, it is necessary to specify the two robots as Robot1 and Robot2, the base coordinate system are named as R_1 and R_2, a calibration tool is installed at both of the robot end-effectors with the name T_1, T_2 respectively (Fig. 2).

The whole calibration process is displayed in Figs. 3 and 4. At the first step, in the two-robot common workspace, the operator adjusts the joint 2 to 6 of Robot2 to move the T_2 to a good position for the contact of T_1 while keep joint1 at 0 angular position, then makes the end of T_1 and T_2 contact at P_1 through adjust the 6 joints of Robot1, records

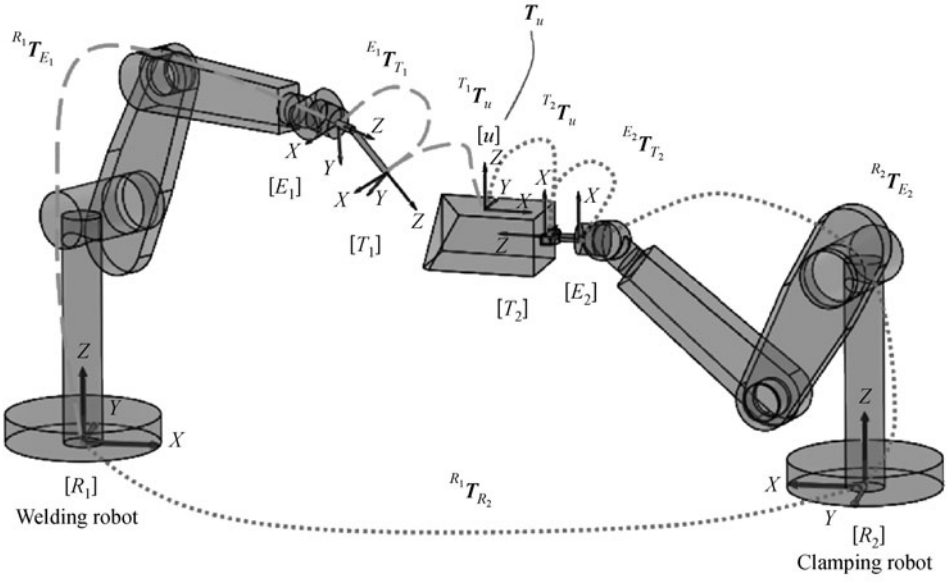

Fig. 1 Dual-robot coordinates system

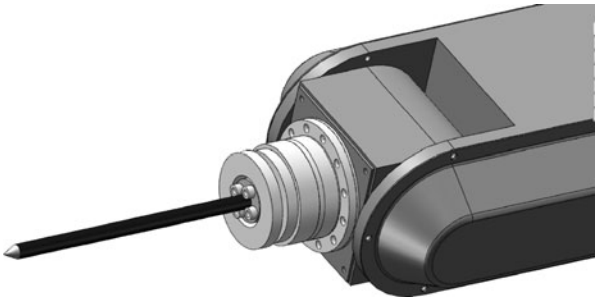

Fig. 2 Calibration tool

the 6 joint angular positions of both robots via reading angular displacements of the joint sensors. At the second step, the operator only rotates the joint 1 of Robot2 for θ, after that does the same operations at step one, makes the end of T_1 and T_2 contact at P_2, record the 6 joint angular positions of both robots. At the final step, the operator only rotates the joint 1 of Robot2 for Φ, makes the end of T_1 and T_2 contact at P_3, record the 6 joint angular positions of both robots.

Now there are three contact points P_1, P_2 and P_3, moreover, an assist coordinate system R_3 is introduced. We can obtain the position and orientation of R_3 origin O_3 in the coordinate system R_1 by the geometric calculation below. And the position and orientation of R_2 origin O_2 in the coordinate system R_1 can also be obtained by the geometric relationship with R_3.

In the coordinate system of R_1, the P_1, P_2, P_3, O_2, O_3 are given as below:

$$P_1(x_1,y_1,z_1),$$

$$P_2(x_2,y_2,z_2),$$

$$P_3(x_3,y_3,z_3),$$

$$O_2(x_{o2},y_{o2},z_{o2}),$$

$$O_3(x_{o3},y_{o3},z_{o3}).$$

The position vectors $\boldsymbol{x}_{o3}$, $\boldsymbol{y}_{o3}$, $\boldsymbol{z}_{o3}$ of O_3, can be obtained by solving plane equations (Fig. 4).

The direction vectors $\boldsymbol{u}$, $\boldsymbol{v}$, $\boldsymbol{w}$ can be obtained by Eqs. (3)–(5).

$$r = \sqrt{(x_1 - x_{o3})^2 + (y_1 - y_{o3})^2 + (z_1 - z_{o3})^2}, \tag{2}$$

$$\boldsymbol{u} = \frac{\overrightarrow{P_0P_1}}{|\overrightarrow{P_0P_1}|}, \tag{3}$$

this is the X axis orientation vector of R_3 coordinate system.

$$\boldsymbol{w} = \frac{\overrightarrow{P_1P_2} \times \overrightarrow{P_2P_3}}{|\overrightarrow{P_1P_2} \times \overrightarrow{P_2P_3}|}, \tag{4}$$

this is the Z axis orientation vector of R_3 coordinate system.

$$\boldsymbol{v} = \boldsymbol{w} \times \boldsymbol{u}, \tag{5}$$

this is the Y axis orientation vector of R_3 coordinate system.

$${}^{R_1}\boldsymbol{T}_{R_3} = \begin{bmatrix} u_x & v_x & w_x & x_{o3} \\ u_y & v_y & w_y & y_{o3} \\ u_z & v_z & w_z & z_{o3} \\ 0 & 0 & 0 & 1 \end{bmatrix}. \tag{6}$$

As the orientation vectors of R_2 and R_3 coordinate system are the same, the only difference of them is origin O_2 moved along the Z axis for distance z_1 relative to O_3. Therefore, the position vectors of O_2 can be obtained by Eq. (7).

$$\boldsymbol{x}_{o2} = \boldsymbol{x}_{o3} + \boldsymbol{w}_x \times \Delta\boldsymbol{z}, \boldsymbol{y}_{o2} = \boldsymbol{y}_{o3} + \boldsymbol{w}_y \times \Delta\boldsymbol{z},$$

$$\boldsymbol{z}_{o2} = \boldsymbol{z}_{o3} + \boldsymbol{w}_z \times \Delta\boldsymbol{z}. \tag{7}$$

In Eq. (7), $\Delta\boldsymbol{z}$ is the Cartesian Z axis position vector of T_2 end in R_2 coordinate system, which can be calculated by the six joint angular displacements read from the joint sensors. Finally, the matrix ${}^{R_1}\boldsymbol{T}_{R_2}$ can be obtained:

$${}^{R_1}\boldsymbol{T}_{R_2} = \begin{bmatrix} u_x & v_x & w_x & x_{o2} \\ u_y & v_y & w_y & y_{o2} \\ u_z & v_z & w_z & z_{o2} \\ 0 & 0 & 0 & 1 \end{bmatrix}. \tag{8}$$

After the matrix ${}^{R_1}\boldsymbol{T}_{R_2}$ is already known, the Cartesian pose matrix of robot end-effector ${}^{R_1}\boldsymbol{T}_{E_1}$ and ${}^{R_2}\boldsymbol{T}_{E_2}$ can be obtained by Eqs. (9) and (10).

$${}^{R_1}\boldsymbol{T}_{E_1} = \boldsymbol{T}_u \times {}^{T_1}\boldsymbol{T}_u^{-1} \times {}^{E_1}\boldsymbol{T}_{T_1}^{-1}, \tag{9}$$

$${}^{R_2}\boldsymbol{T}_{E_2} = {}^{R_1}\boldsymbol{T}_{R_2}^{-1} \times \boldsymbol{T}_u \times {}^{T_2}\boldsymbol{T}_u^{-1} \times {}^{E_2}\boldsymbol{T}_{T_2}^{-1}. \tag{10}$$

Finally, the six joint displacements can be calculated by inverse kinematics.

2.3 Inverse kinematics

For 6-DOF industrial robots similar to Puma560. When the robot end-effecter pose in Cartesian space is known, the process of analytical method for solving inverse kinematics of six joint angular displacements (θ_1, θ_2, θ_3, θ_4, θ_5, θ_6) can refer to Ref. [16]. This paper only makes use of the final analytical inverse equations based on the parameters of the 6-DOF robot used in the school's laboratory. Among the six joint angular displacements, there are two solutions

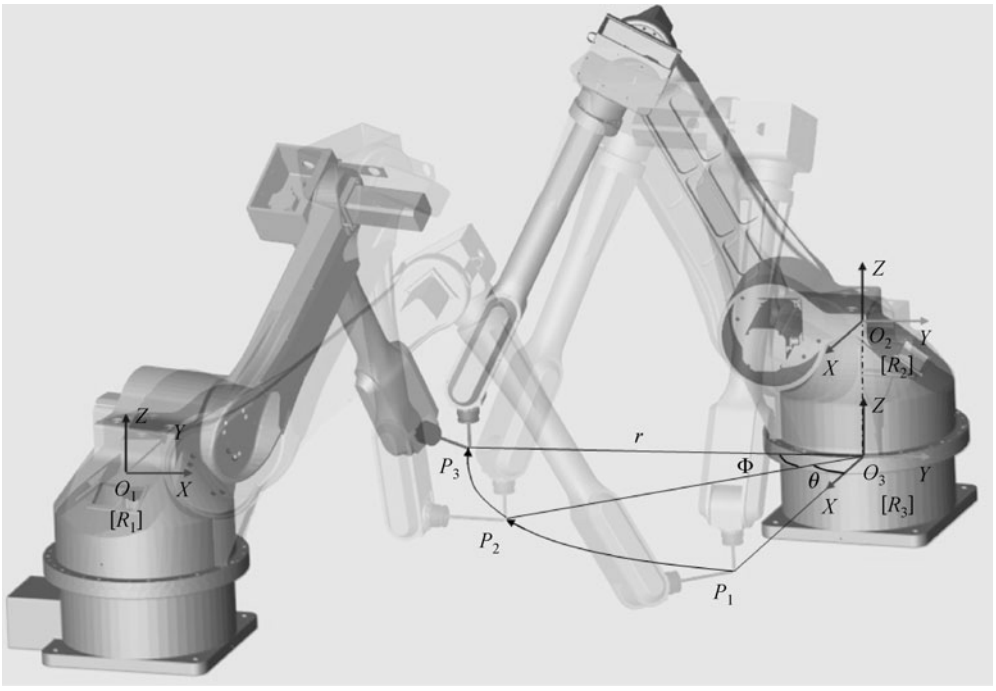

Fig. 3 Three-point calibration process

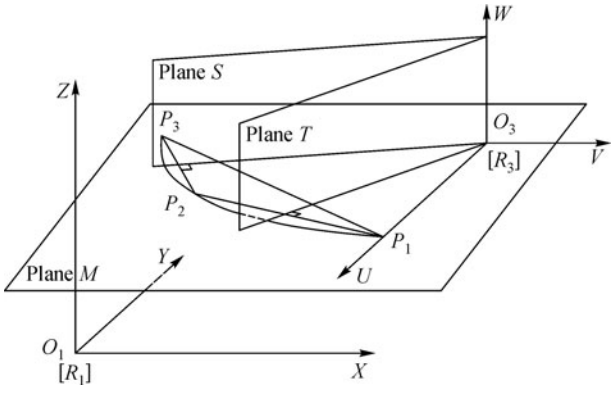

Fig. 4 Three-point calibration coordinate systems and parameters

for θ_1 and θ_2, if θ_1 is selected, θ_2 and θ_3 may have solution of two groups. If θ_1, θ_2, θ_3 are selected, θ_4, θ_5, θ_6 have two groups of solution. Therefore, the robot analytical inverse kinematics solution may have up to eight groups. There are mainly three principles when choosing the best group. Firstly, it should be ensured that all joints did not exceed the maximum working range; and for the second, is to avoid collision between robots or between robot and the environment; and the final one, for the consideration of minimum energy consumption and motion stabilization, the entire movement change of the six joint angular displacements should be weighted minimum.

3 Two-robot coordinated motion planning and simulation platform establishment

There are two types of motion planning for two-robot coordination. Which are master/slave mode and non master/slave mode [17]. Since the spatial seam is complex, this paper chooses the non master/slave mode to ease the seam description and increase the intuitive. The non master/slave mode sets the pose versus time function of a point u on the object, the tool end paths of welding robot (Robot1) and the clamping robot (Robot2) can be obtained by the constrained relationships between the object and each robot respectively. After that, the 6 joint angular displacement values of each robot can be resolved by inverse kinematics. As shown in Fig. 5, $[{}^{T_1}\boldsymbol{T}_u]^{-1}$, $[{}^{T_2}\boldsymbol{T}_u]^{-1}$ are the specified constrained relationship matrixes, ${}^{R1}\boldsymbol{T}_{E_1}$, ${}^{R_2}\boldsymbol{T}_{E_2}$ are constant transformation matrixes between the robot end-effecter and the tool, which can be obtained according to Eqs. (9) and (10).

This paper use Solidworks-SimMechanics as the tool for establishing the simulation platform. The origin robot model is the 6-DOF robot used in the school's laboratory. The parameters of the robot is listed in Table 1.

The modeling process includes:

1) Establishing the 3D model of two-robot system in Solidworks (Fig. 6).

2) Downloading the SimMechanics Link plug-in component from the Mathworks official website, and installing it to Solidworks by Matlab command.

Table 1 Parameters of robot

i	α_{i-1}	a_{i-1}	d_i	θ_i	Working range	Max speed
1	0	0	0	θ_1	±180º	90º/s
2	−90°	a_1	0	θ_2	−120º–70º	90º/s
3	0	a_2	d_3	θ_3	−70º–220º	90º/s
4	−90°	a_3	d_4	θ_4	±350º	110º/s
5	90°	0	0	θ_5	±130º	110º/s
6	−90°	0	0	θ_6	±355º	200º/s
Parameters	$a_1 = 250$	$a_2 = 875$	$a_3 = 31$	$d_3 = 0$	$d_4 = 1100$	

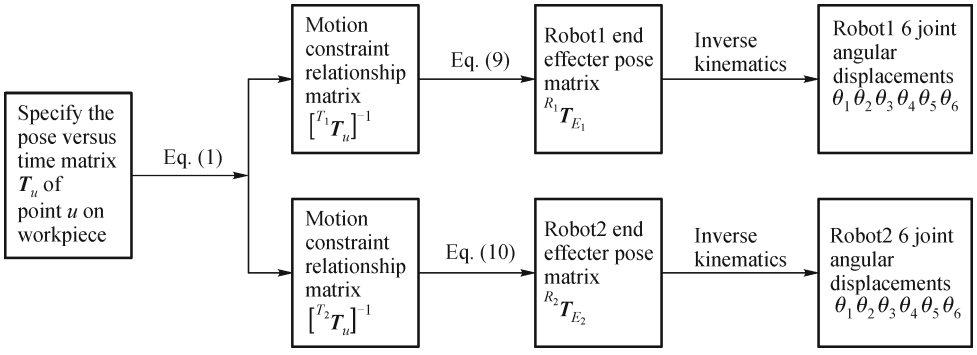

Fig. 5 Coordinated motion planning process

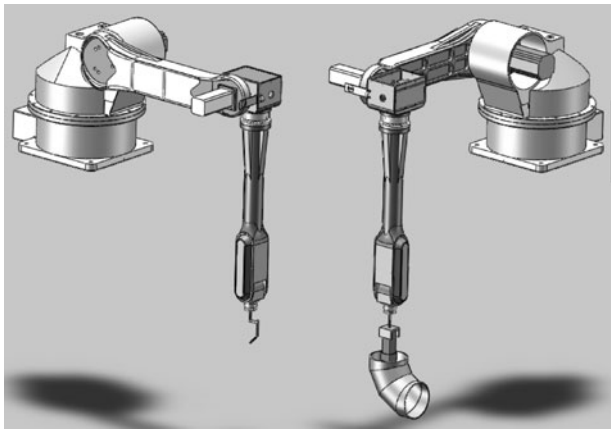

Fig. 6 3D model established in Solidworks

3) Saving the Solidworks models established in step 1 as 'xml' documents (SimMechanics Link documents).

4) Importing the 'xml' documents as a new model in matlab, the SimMechanics model can be generated automatically. The three strings of modules are Robot1, Robot2 and the connection to the Ground (Fig. 7).

5) Adding S-functions, joint actuators, sensors and scopes to the SimMechanics model, realize the actuation and simulation of the model. The system structure is shown in Fig. 8. This simulation system can output 3D motion simulation, tool end trajectories of each robot in Cartesian space and joint sensor information.

4 Simulation platform establishment and task design

For the spatial curve seam, in order to achieve continuous seam tracing, the clamping robot must continuous move the seam point to the ideal position in order to fulfill the requirement of downhand welding [18]. The downhand welding constraints means the normal direction of the seam should against the direction of gravity in every moment. In this process, there are not only relative pose constraints, but also relative motion constraints between the torch and the seam. The relative pose (position and orientation) constraints require that the weld torch to maintain a certain posture which can not be divorced from the seam; Motion constraints require the weld torch and the seam to meet certain relative movement constrains. In this regard, this paper using downhand welding constraints, two-robot motion coordination and kinematics analysis in the welding process.

This paper chooses a steel curved pipe, which is widely used in petrochemical and coal industry, as the workpiece for two-robot coordinated welding. The steel curved pipe consists of 4 sections that are shown in Figs. 9 and 10 show the dimensions.

As the welding seam is oval, the welding task need to divided into two sections, or else, the fourth joint of clamping robot will be out of maximum working range. Therefore, the whole oval seam is divided into two semi-elliptical arcs. The two-robot finish the seam welding of

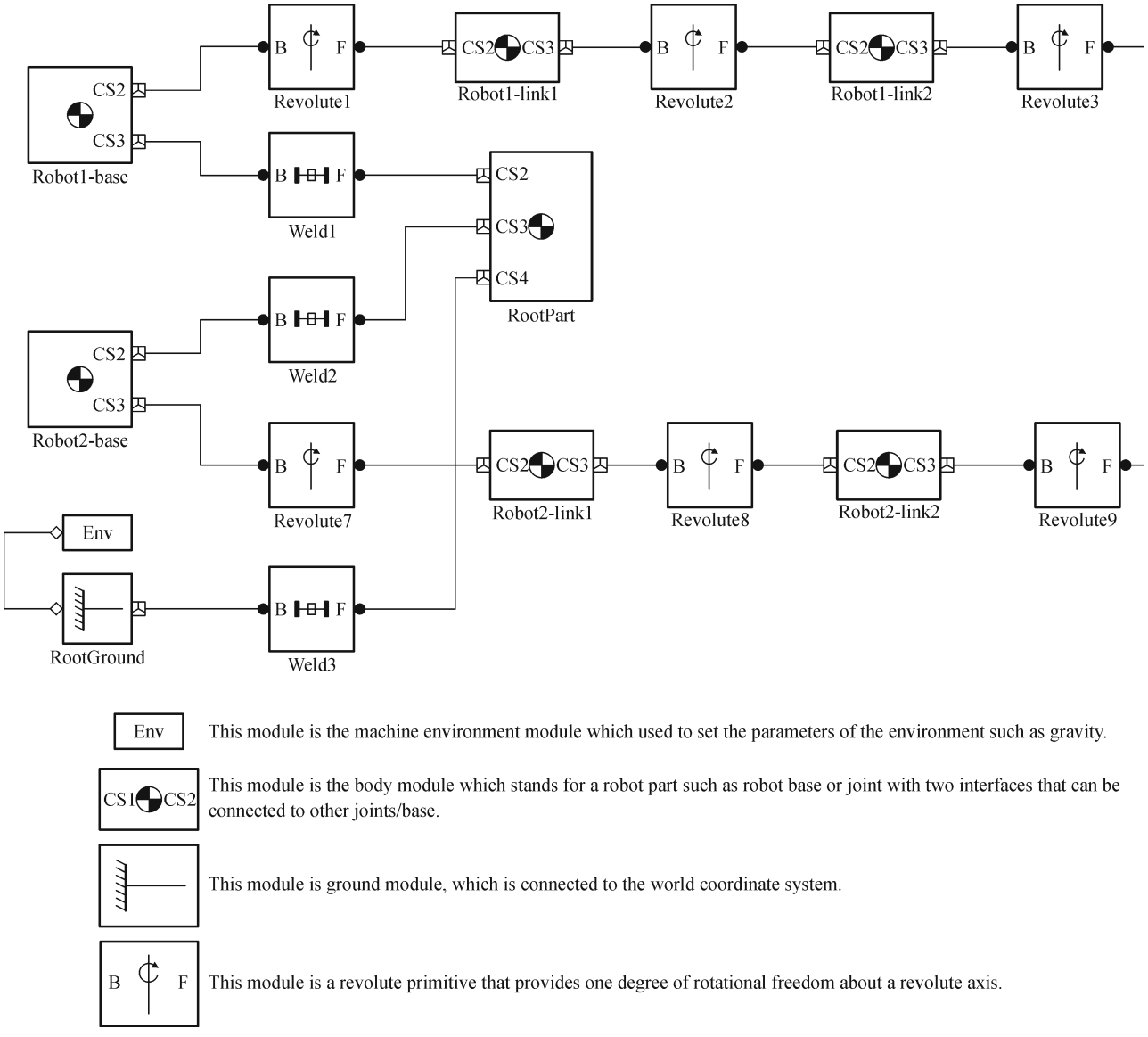

Fig. 7 SimMechanics model

first semi-elliptical arc (clockwise), after that, both of the two robots move back to the starting position, then the second semi-elliptical arc welding is executed, the whole welding task design is shown in Fig. 11.

Parameter m is the anger between the X-axis of coordinate system $[u]$ and the seam cross section (see Fig. 10), R, d, α, x_{u2}, y_{u2}, z_{u2} is shown in Figs. 9 and 10. We can obtain the following matrices, fixed angle coordinate system is used for rotation matrix, and u is set to be the circle center of the steel right-angle bend pipe in the XY plane. Simulation running time is set to a constant T, the time variable $t \in [0, T]$. $\boldsymbol{T}_m$ is the rotational angle of welding torch relative to the X axis of base coordinate system R_1, which is a rotation compensation matrix, in order to adjust the working plane of torch to coincide with the plane of the seam. Since the welding task is divided into two sections, the simulation model of Fig. 8 need to modified, the modified model is shown in Fig. 13.

$$\boldsymbol{T}_m = \begin{pmatrix} \cos(m \times \pi/180) & -\sin(m \times \pi/180) & 0 & 0 \\ \sin(m \times \pi/180) & \cos(m \times \pi/180) & 0 & 0 \\ 0 & 0 & 0 & 0 \\ 0 & 0 & 0 & 1 \end{pmatrix}, \tag{11}$$

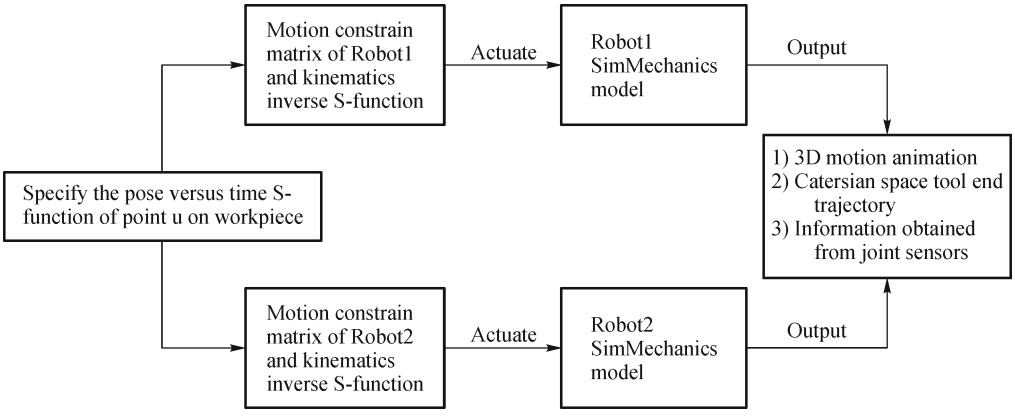

Fig. 8 Solidworks-SimMechanics simulation model structure

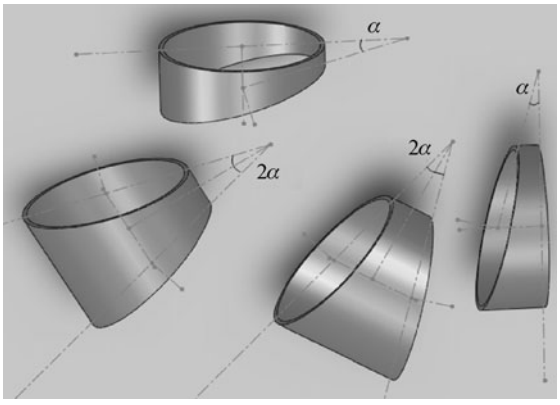

Fig. 9 Steel curved pipe structure

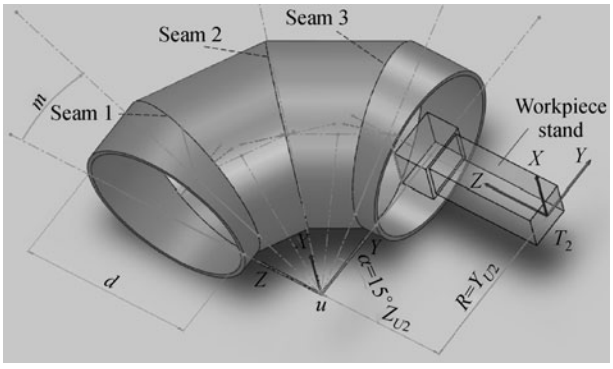

Fig. 10 Dimensions of steel curved pipe

$$\left[{}^{T_1}\boldsymbol{T}_u\right]^{-1}{}_{\text{clockwise}} = \boldsymbol{T}_m \times \begin{pmatrix} & & R/\cos\alpha - \cos(\pi t/T)d/(2\cos\alpha) \\ Y(\pi/2+\pi t/T) & & 0 \\ & & \sin(\pi t/T)d/2 \\ 0 \quad 0 \quad 0 & & 1 \end{pmatrix}, \tag{12}$$

$$\left[{}^{T1}\boldsymbol{T}_u\right]^{-1}{}_{\text{counter-clockwise}} = \boldsymbol{T}_m \times \begin{pmatrix} & & R/\cos\alpha + \cos(\pi t/T)d/(2\cos\alpha) \\ Y(\pi t/T)Y(\pi/2)X(\pi) & & 0 \\ & & -\sin(\pi t/T)d/2 \\ 0 \quad 0 \quad 0 & & 1 \end{pmatrix}, \tag{13}$$

$$\left[{}^{T_2}\boldsymbol{T}_u\right]^{-1} = \begin{pmatrix} 1 & 0 & 0 & u_{xu2} \\ 0 & 1 & 0 & u_{yu2} \\ 0 & 0 & 1 & u_{zu2} \\ 0 & 0 & 0 & 1 \end{pmatrix}. \tag{14}$$

5 Calibration and motion simulation

5.1 Calibration

Use the claibration method described in Sect. 1.2, the record of the three-point calibration is illustrated in Tables 2 and 3.

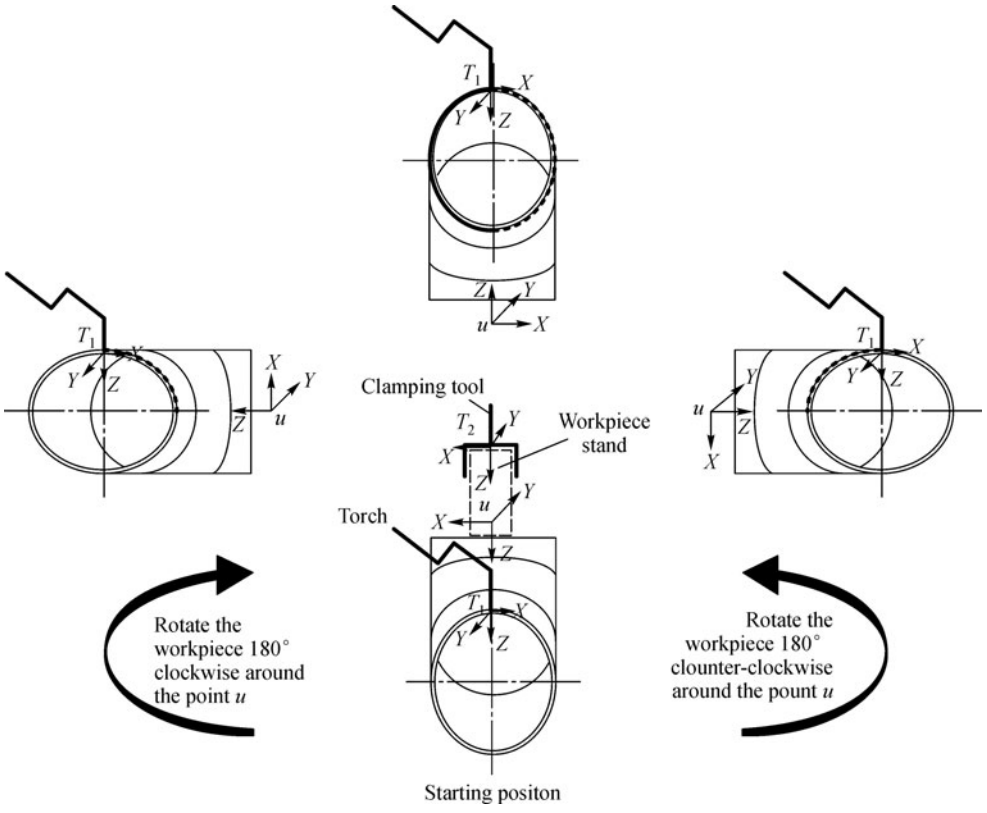

Fig. 11 Coordinated welding task design

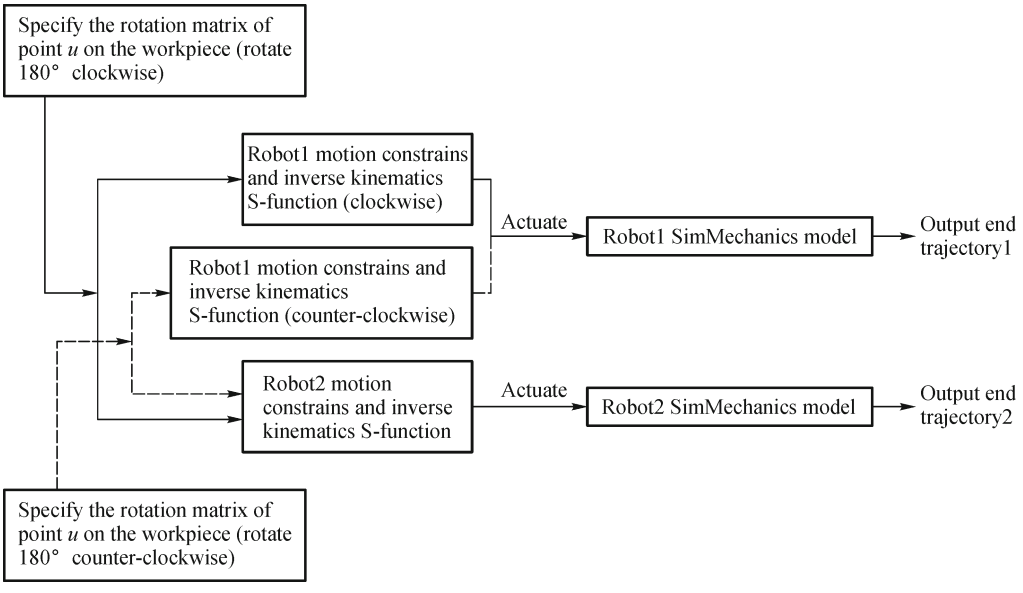

Fig. 12 Modified steel curved pipe simulation model

According to the Eqs. (2)–(8), the position vectors and orientation vectors of $\boldsymbol{O}_3$ can be obtained.

$\boldsymbol{P}_1(x_1, y_1, z_1) = (1700, 450, -400)$,

$\boldsymbol{P}_2(x_2, y_2, z_2) = (851.469, 801.472, -400)$,

$\boldsymbol{P}_3(x_3, y_3, z_3) = (518.228, 1141.624, -400)$,

$\boldsymbol{O}_3(x_{o3}, y_{o3}, z_{o3}) = (1700, 1650, -400)$,

$$r = \sqrt{(x_1 - x_{o3})^2 + (y_1 - y_{o3})^2 + (z_1 - z_{o3})^2} = 1200,$$

$\boldsymbol{u} = (0, -1, 0)$, $\boldsymbol{w} = (0, 0, -1)$, $\boldsymbol{v} = \boldsymbol{w} \times \boldsymbol{u} = (-1,0,0)$,

Table 2 Calibration information of Robot1

Calibration point	Robot1 tool end position in coordinate system R_1/mm			6 joint angular displacements/(º)					
	X	Y	Z	θ_1	θ_2	θ_3	θ_4	θ_5	θ_6
$\boldsymbol{P}_1$	1699.99795	449.99795	−400	9.016	−38.324	8.8706	140.1757	66.554	−67.9868
$\boldsymbol{P}_2$	851.46909	801.472	−400	55.6151	−51.623	43.9317	−124.144	85.665	−96.3598
$\boldsymbol{P}_3$	518.22762	1441.62367	−400	80.5105	−33.445	−1.6449	−68.671	104.3345	−141.041

Table 3 Calibration information of Robot2

Calibration point	Robot2 tool end position in coordinate system R_2/mm			6 joint angular displacements/(º)					
	X	Y	Z (Δz)	θ_1	θ_2	θ_3	θ_4	θ_5	θ_6
$\boldsymbol{P}_1$	1200	0	−400	0	−61.7759	34.22983	0	27.54609	0
$\boldsymbol{P}_2$	848.528	−848.528	−400	−45	−61.7759	34.22984	0	27.54609	0
$\boldsymbol{P}_3$	208.378	−1181.77	−400	−80	−61.7759	34.22978	0	27.54611	0

$$
{}^{R_1}\boldsymbol{T}_{R_3} = \begin{bmatrix} u_x & v_x & w_x & x_{o3} \\ u_y & v_y & w_y & y_{o3} \\ u_z & v_z & w_z & z_{o3} \\ 0 & 0 & 0 & 1 \end{bmatrix}
$$

$$
= \begin{bmatrix} 0 & -1 & 0 & 1700 \\ -1 & 0 & 0 & 1650 \\ 0 & 0 & -1 & -400 \\ 0 & 0 & 0 & 1 \end{bmatrix},
$$

$$
\Delta z = -400, \text{ (Table 3)}
$$

$$
x_{o2} = x_{o3} + w_x \times \Delta z = 1700,
$$

$$
y_{o2} = y_{o3} + w_y \times \Delta z = 1650,
$$

$$
z_{o2} = z_{o3} + w_z \times \Delta z = 0.
$$

Obtain $\boldsymbol{O}_2(x_{o2}, y_{o2}, z_{o2}) = (1700, 1650, 0)$. Finally,

$$
{}^{R_1}\boldsymbol{T}_{R_2} = \begin{bmatrix} u_x & v_x & w_x & x_{o2} \\ u_y & v_y & w_y & y_{o2} \\ u_z & v_z & w_z & z_{o2} \\ 0 & 0 & 0 & 1 \end{bmatrix}
$$

$$
= \begin{bmatrix} 0 & -1 & 0 & 1700 \\ -1 & 0 & 0 & 1650 \\ 0 & 0 & -1 & 0 \\ 0 & 0 & 0 & 1 \end{bmatrix}, \tag{15}
$$

5.2 Motion simulation

In Fig. 11, the angle m of seam 1,2,3 is 15º, 45º and 75º, respectly. α = 15º, ${}^{E_1}\boldsymbol{T}_{T_1}$, ${}^{E_2}\boldsymbol{T}_{T_2}$ are constant matrices decided by the tooles installed. Choose the seam 2 for the coordinated welding simulation. Simulation time is set as T = 20 s.

$$
{}^{E_1}\boldsymbol{T}_{T_1} = \begin{pmatrix} 0.7071 & 0 & -0.7071 & 0 \\ 0 & 1 & 0 & 0 \\ 0.7071 & 0 & 0.7071 & 303 \\ 0 & 0 & 0 & 1 \end{pmatrix},
$$

$$
{}^{E2}\boldsymbol{T}_{T_2} = \begin{pmatrix} 1 & 0 & 0 & 0 \\ 0 & 1 & 0 & 0 \\ 0 & 0 & 1 & 210 \\ 0 & 0 & 0 & 1 \end{pmatrix}. \tag{16}
$$

According to Eqs. (10)–(13) and (16), the S-function matrix parameters of the two-robot model can be set according to these matrixes, and then you can run the model for the simulation. View from the motion animation, the welding process is uniform and stable, welding torch and the seam keep close fit at any time and keep a constant welding angle, which can meet the requirements of downhand welding, there is no collision during the welding process (Fig. 13).

Due to the limitation of the pages, only the tool end trajectories of clockwise rotation are given. Meanwhile, six joint displacement, angular velocity and acceleration of the Robot2 (clockwise) are given.

The Cartesian trajectory curves of the tool ends (Fig. 14)

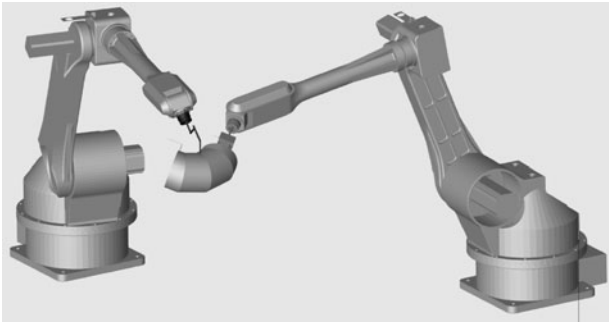

Fig. 13 Two-robot coordinated welding simulation

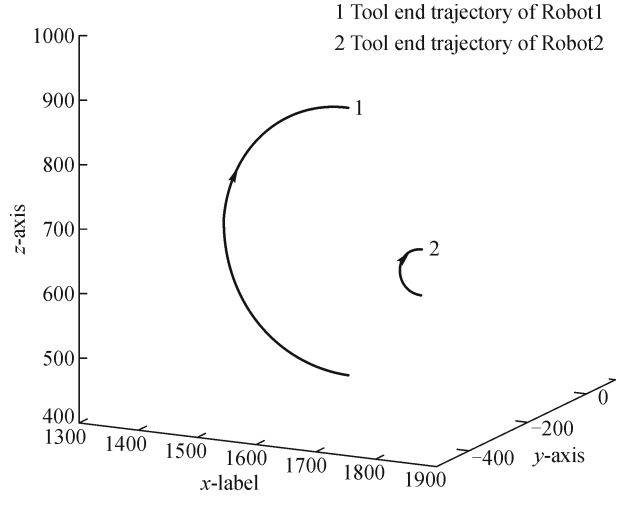

Fig. 14 Tool end trajectories of clocewise rotation

show that both of the tool end trajectory curves are plane arc and the curves are smooth and continuous.

Figure 15 shows that the curves of six joint angular displacements are smooth and continuous, no joint angular displacement exceeds the working scope. However, as the analytical inverse kinematics has employed the function 'atan2', this function output the only result in the range of angle (-180^o, 180^o), therefore, if the angular displacement of joint movement exceeds this range, the angular displacement curve may have 180^o abrupt change. This phenomenon happened in θ_4 of Robot2 (Fig. 15). Correct solution should be $\theta_4 - 180^o$. Figures 16 and 17 illustrate that there are abrupt changes in the initial angular velocity and acceleration as there is no transition curve before the starting of the task, which can be improved by adding transition curves before task starting and after task termination. Some motion planning optimization can also be helpful for finding such as time-optimal or energy-optimal trajectory which is not included here.

6 Conclusions

This paper has analysed two 6-DOF industrial robot welding coordination that one robot grips the workpiece to be welded while the other robot implements the welding task.

The three-point calibration method is described in details which can obtain the base coordinate system transformation matrix between two robots in practical. View from the steel curved pipe motion animation, the welding process can meet the requirements of downhand welding, and there is no collision during the welding process. The six joint angular displacement curves are smooth and continuous, no joint velocities are out of working scope. However, there are abrupt changes in the initial angular velocity and acceleration as there is no transition curve at the beginning and the end, which can be improved by adding transition curves before task starting and after task termination.

This dual-robot coordinated welding simulation system can be helpful of off-line motion planning of complex seam task design, motion planning and early detection of problems such as joint displacement, velocity limitation

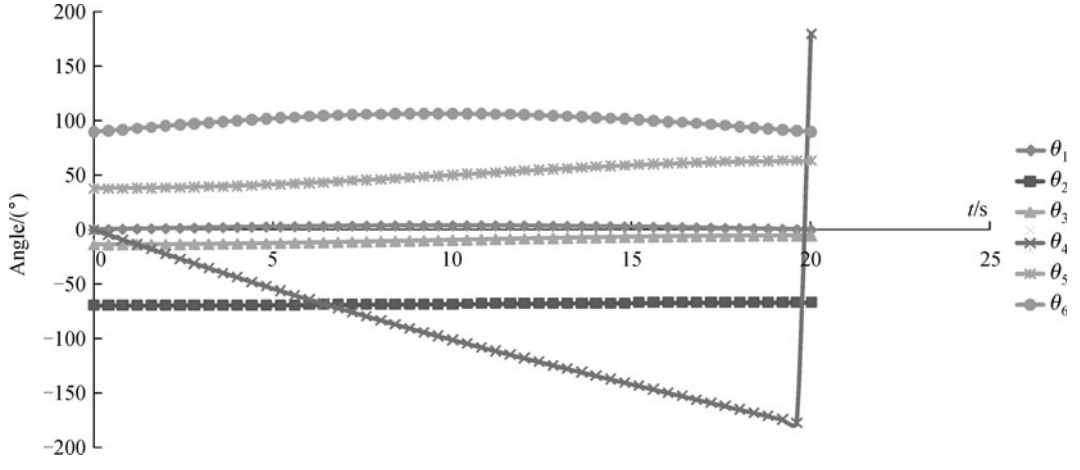

Fig. 15 Six joint displacement curves of Robot2 (clockwise rotation)

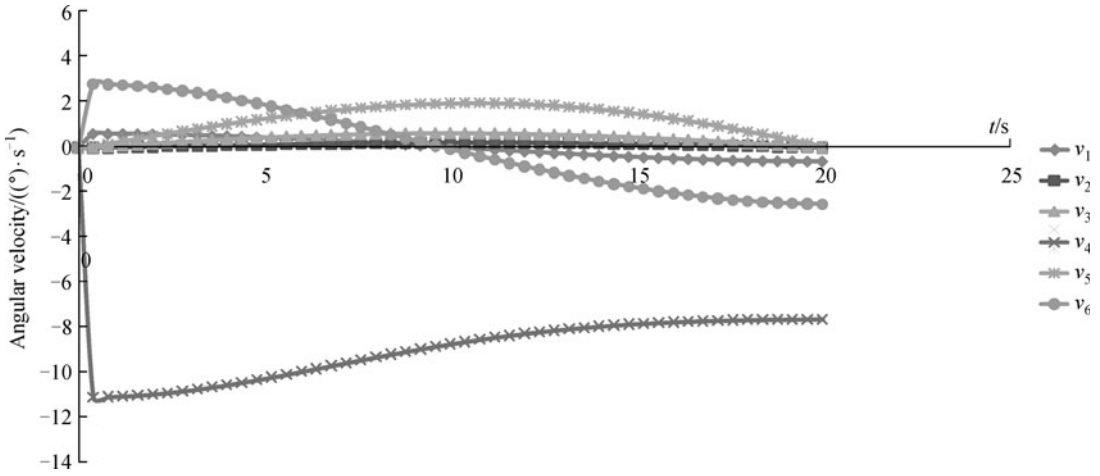

Fig. 16 Six joint angular velocity curves of Robot2 (clockwise rotation)

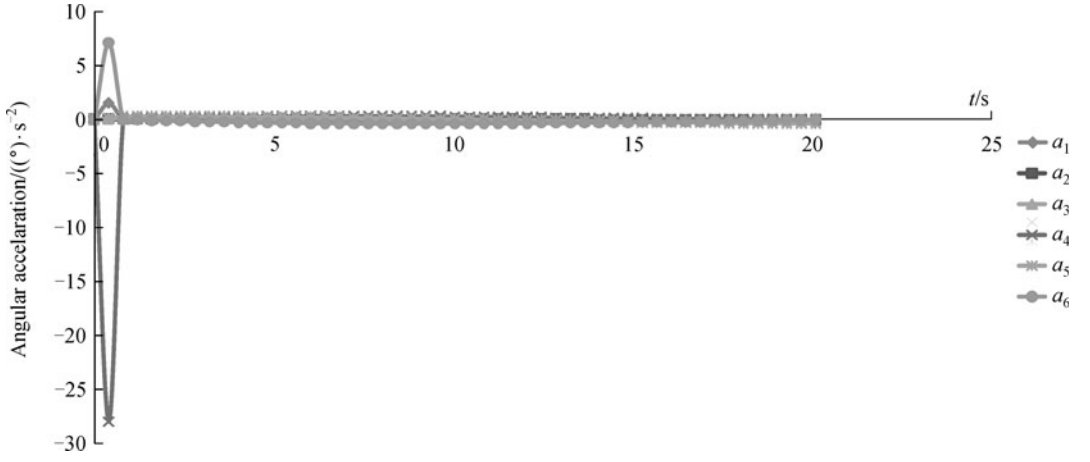

Fig. 17 Six angular accelaration curves of Robot2 (clockwise rotation)

and collision. However, one limitation of this two-robot system is that the seam should be expressed as accurate mathematical formula which might be difficult in practical. Moreover, this article focuses on the coordinated motion planning and system simulation, other issues such as trajectory optimization, errors from assembly and error compensation is not involved.

Acknowledgements This work was partly supported by the National High Technology Research and Development Key Program of China (No. 2009AA043901–3), Breakthrough Projects Focused on Key Areas of Hong Kong and Guangdong (No. 20090101-1), Science and Technology Planning Project of Guangdong Province (No. 2010B080703004) and Industry, University and Research Project of Guangdong Province (No. 2010B090400259).

References

1. Jouaneh M K, Wang Z, Dornfeld D A. Trajectory planning for coordinated motion of a robot and a positioning table. I. Path specification. IEEE Transactions on Robotics and Automation, 1990, 6(6): 735–745
2. Chien Y P, Xue Q, Chen Y. Configuration space model of tightly coordinated two robot manipulators operating in 3-dimensional workspace. IEEE International Conference on Systems, Man and Cybernetics, 1992, 2: 1110–1115
3. Lee B H, Lee C S G. Collision-free motion planning of two robots. IEEE Transactions on Systems, Man and Cybernetics, 1987, 17(1): 21–32
4. Chang C, Chung M J, Lee B H. Collision avoidance of two general robot manipulators by minimum delay time. IEEE Transactions on Systems, Man and Cybernetics, 1994, 24(3): 517–522
5. Bien Z, Lee J. A minimum-time trajectory planning method for two robots. IEEE Transactions on Robotics and Automation, 1992, 8(3): 414–418
6. Hwang K S, Ju M Y, Chen Y J. Speed alteration strategy for multijoint robots in co-working environment. IEEE Transactions on Industrial Electronics, 2003, 50(2): 385–393
7. Shin Y S, Bien Z. A novel method of collision-free trajectory planning for two robot arms. In: Proceedings of the 1988 IEEE

International Conference on Systems, Man, and Cybernetics, 1988, 2: 791–794

8. Chiddarwar S S, Babu N R. Dynamic priority allocation for conflict free coordinated manipulation of multiple agents. IEEE International Conference on Automation Science and Engineering, 2009, 549–554
9. Yeo H J, Lee S J, Suh I H, Yi B J, Oh S R. External force control using cooperating two arms with general kinematic structures. 5th IEEE International Workshop on Robot and Human Communication, 1996, 388–394
10. Tao J M, Luh J Y S, Zheng Y F. Compliant coordination control of two moving industrial robots. IEEE Transactions on Robotics and Automation, 1990, 6(3): 322–330
11. Yeo H J, Suh II H, Yi B J, Oh S R. A single closed-loop kinematic chain approach for a hybrid control of two cooperating arms with a passive joint: an application to sawing task. IEEE Transactions on Robotics and Automation, 1999, 15(1): 141–151
12. Kraus W J, McCarragher B J. Hybrid position/force coordination for dual-arm manipulation of flexible materials. In: Proceedings of the 1997 IEEE/RSJ International Conference on Intelligent Robots and Systems, 1997, 1: 202–207
13. Cho H K, Kim J, Yea S H. Task-oriented path planning for the coordinated motion of two manipulators. In: Proceedings of the 6th IEEE International Workshop on Robot and Human Communication, 1997, 46–50
14. Kasagami F, Ishimatsu T, Watanabe S, Izawa A, Koujina Y. Coordinated motion of arc welding robots using parallel data processor. In: Proceedings of the 1992 International Conference on Power Electronics and Motion Control, 1992, 2: 656–663
15. Tang C Q, Meng Z D. Realization of coordinated motion of arc-robot and positioned. Industrial Control Computer, 2008, 21(1): 47–49 (in Chinese)
16. Craig J J. Introduction to Robotics: Mechanics and Control. 3rd ed. Saddle River: Prentice Hall, 2004
17. Wu L, Cui K, Chen S B. Redundancy coordination of multiple robotic devices for welding through genetic algorithm. Robotica, 2000, 18(6): 669–676
18. Fernandez K, Cook E. A generalized method for automatic downhand and wirefeed control of a welding robot and positioned. NASA technical paper 2807, 1988